articles

molecular pharmaceutics

# Peptide-Conjugated PAMAM for Targeted Doxorubicin Delivery to Transferrin Receptor Overexpressed Tumors

**Liang Han, Rongqin Huang, Shuhuan Liu, Shixian Huang, and Chen Jiang***

*Department of Pharmaceutics, School of Pharmacy, Fudan University, Shanghai, China*

Received May 31, 2010; Revised Manuscript Received August 20, 2010; Accepted September 21, 2010

**Abstract:** The purpose of this work was to evaluate the potential of HAIYPRH (T7) peptide as a ligand for constructing tumor-targeting drug delivery systems. T7 could target to transferrin-receptor (TfR) through a cavity on the surface of TfR and then transport into cells via endocytosis with the help of transferrin (Tf). In this study, T7-conjugated poly(ethylene glycol) (PEG)-modified polyamidoamine dendrimer (PAMAM) (PAMAM-PEG-T7) was successfully synthesized and further loaded with doxorubicin (DOX), formulating PAMAM-PEG-T7/DOX nanoparticles (NPs). In vitro, almost 100% of DOX was released during 2 h in pH 5.5, while only 55% of DOX was released over 48 h in pH 7.4. The cellular uptake of DOX could be significantly enhanced when treated with T7-modified NPs in the presence of Tf. Also, the in vitro antitumor effect was enhanced markedly. The $IC_{50}$ of PAMAM-PEG-T7/DOX NPs with Tf was 231.5 nM, while that of NPs without Tf was 676.7 nM. T7-modified NPs could significantly enhance DOX accumulation in the tumor by approximately 1.7-fold compared to that of unmodified ones and by approximately 5.3-fold compared to that of free DOX. For in vivo antitumor studies, tumor growth of mice treated with PAMAM-PEG-T7/DOX NPs was significantly inhibited compared to that of mice treated with PAMAM-PEG/DOX NPs and saline. The study provides evidence that PAMAM-PEG-T7 can be applied as a potential tumor-targeting drug delivery system. T7 may be a promising ligand for targeted drug delivery to the tumor.

**Keywords:** Doxorubicin; PAMAM; HAIYPRH; tumor-targeting; enhanced permeability and retention; receptor-mediated endocytosis

## Introduction

Targeting and killing of tumor cells via chemotherapy is considered to be very effective to inhibit the growth of tumor cells. However, the applications of current drug delivery systems are limited due to their poor targeting efficiency and apparent side effects.

As known, the strategies for the design of tumor targeting drug delivery systems were mainly based on the effect of enhanced permeability and retention (EPR) and the mechanism of receptor-mediated endocytosis. The effect of EPR is thought to be useful for the targeting of the macromolecular drugs to the tumor tissues on a vasculolymphatic level.[1] It has been proven applicable for most tumors and utilized in designing cancer-targeting drug delivery systems such as macromolecular, micellar, and lipidic particles.[2−5] On the other hand, ligand-mediated drug delivery has been proven as a more active tumor-targeting strategy for specifically recognizing the tumor cells and trafficking into cells

* To whom correspondence should be addressed. Mailing address: Chen Jiang, Ph.D., Professor, Department of Pharmaceutics, School of Pharmacy, Fudan University, 826 Zhangheng Road, Shanghai 201203, China. Telephone: (86) 21-51980079. Fax: (86) 21-51980079. E-mail: jiangchen@shmu.edu.cn.

(1) Tanaka, T.; Shiramoto, S.; Miyashita, M.; Fujishima, Y.; Kaneo, Y. Tumor targeting based on the effect of enhanced permeability and retention (EPR) and the mechanism of receptor-mediated endocytosis (RME). *Int. J. Pharm.* **2004**, *277* (1−2), 39–61.

(2) Matsumura, Y.; Maeda, H. A new concept for macromolecular therapeutics in cancer chemotherapy: mechanism of tumoritropic accumulation of proteins and the antitumor agent smancs. *Cancer Res.* **1986**, *46* (12 Pt 1), 6387–6392.

(3) Maeda, H.; Matsumura, Y. Tumoritropic and lymphotropic principles of macromolecular drugs. *Crit. Rev. Ther. Drug Carrier Syst.* **1989**, *6* (3), 193–210.



**10.1021/mp100185f** 
Published on Web 09/21/2010

by receptor-mediated endocytosis. This active mechanism might greatly promote the cellular uptake of the delivery systems after their accumulation in tumor tissues.[6] Many receptors have been reported to be overexpressed on the surface of tumor cells, including transferrin-receptor (TfR),[7] epidermal growth factor receptor,[8] and vascular endothelial growth factor receptor-2.[9] These receptors are related to growth and survival of cells, and could implement signal transduction via triggering endocytosis. With overexpressed receptors on tumor cells as targets, ligand-modified delivery systems are designed to enhance the drug accumulation in tumor tissues. Many tumor-targeting ligands have already been tested for targeting delivery, including galactose,[10] asialoorosomucoid,[11,12] folate,[13] transferrin (Tf),[7] and insulin.[14,15]

TfR has been reported to be overexpressed on tumor cells, about 100-fold more than that on normal cells, due to the urgent requirement of iron to maintain cellular survival. Binding of iron-loaded Tf to TfR triggers endocytosis and then the Tf−TfR complex enters cells to provide iron. The feasibility of Tf as a targeting ligand has been demonstrated.[7,16,17] However, the concentration of endogenous Tf in blood (25 $\mu$M) is very high, compared with the $K_d$ of Tf binding to TfR. The endogenous Tf may competitively inhibit the binding of Tf-modified drug delivery systems to TfR; in addition, the relatively high molar weight of Tf, about 80 kDa, makes it difficult for the construction of drug delivery systems.

A unique targeting agent under investigation currently is HAIYPRH, designated as T7, first screened by a phage display system on the cells expressing human TfR.[18] Besides the high affinity for TfR ($K_d$ of ~10 nM), that the binding site of T7 to TfR is different from that of Tf to TfR is more advantageous.[19] Thus, endogenous Tf would not inhibit the uptake of T7-modified drug delivery systems; on the contrary, endogenous Tf in vivo could promote the uptake of T7,[19] showing great potential of T7 as a ligand targeting TfR overexpressed tumors. It has been reported that T7-artemisinin conjugate showed markedly improved efficacy ($IC_{50}$ of the conjugate was 4.7-fold lower than that of free artemisinin against leukemia cells) and selectivity ($IC_{50}$ > 10 000 $\mu$M against normal leukocytes).[19] However, all previous studies involving T7 were focused on in vitro targeting efficiency at the cell level.[18,19] So far, little literature about, in vivo, how much T7-modified systems can specifically accumulate in tumors is found. In this study, T7 was used as a ligand for delivering drug to transferrin receptor overexpressed tumor, and the in vivo targeting efficiency is investigated.

Dendrimers are globular, highly branched macromolecules possessing a well-defined core, an interior region, and a large number of end groups. The physical characteristics of dendrimers, including their monodispersity, water solubility, encapsulation ability, and large number of functional peripheral groups, make these macromolecules ideal candidates for drug delivery.[20,21] A dendrimer acts as a unimolecular micelle by encapsulating pharmaceuticals through the forma-

(4) Maeda, H.; Sawa, T.; Konno, T. Mechanism of tumor-targeted delivery of macromolecular drugs, including the EPR effect in solid tumor and clinical overview of the prototype polymeric drug SMANCS. *J. Controlled Release* **2001**, *74* (1−3), 47–61.

(5) Greish, K.; Fang, J.; Inutsuka, T.; Nagamitsu, A.; Maeda, H. Macromolecular therapeutics: advantages and prospects with special emphasis on solid tumour targeting. *Clin. Pharmacokinet.* **2003**, *42* (13), 1089–1105.

(6) Xu, Z.; Gu, W.; Huang, J.; Sui, H.; Zhou, Z.; Yang, Y.; Yan, Z.; Li, Y. In vitro and in vivo evaluation of actively targetable nanoparticles for paclitaxel delivery. *Int. J. Pharm.* **2005**, *288* (2), 361–368.

(7) Wagner, E.; Zenke, M.; Cotton, M.; Beug, H.; Birnstiel, M. L. Transferrin-polycation conjugates as carriers for DNA uptake into cells. *Proc. Natl. Acad. Sci. U.S.A.* **1990**, *87* (9), 3410–3414.

(8) Schiffer, E.; Housset, C.; Cacheux, W.; Wendum, D.; Desbois-Mouthon, C.; Rey, C.; Clergue, F.; Poupon, R.; Barbu, V.; Rosmorduc, O. Gefitinib, an EGFR inhibitor, prevents hepatocellular carcinoma development in the rat liver with cirrhosis. *Hepatology* **2005**, *41* (2), 307–314.

(9) Roth, P.; Hammer, C.; Piguet, A. C.; Ledermann, M.; Dufour, J. F.; Waelti, E. Effects on hepatocellular carcinoma of doxorubicin-loaded immunoliposomes designed to target the VEGFR-2. *J. Drug Targeting* **2007**, *15* (9), 623–631.

(10) Gao, S.; Chen, J.; Xu, X.; Ding, Z.; Yang, Y. H.; Hua, Z.; Zhang, J. Galactosylated low molecular weight chitosan as DNA carrier for hepatocyte-targeting. *Int. J. Pharm.* **2003**, *255* (1−2), 57–68.

(11) Singh, M.; Kisoon, N.; Ariatti, M. Receptor-mediated gene delivery to HepG2 cells by ternary assemblies containing cationic liposomes and cationized asialoorosomucoid. *Drug Delivery* **2001**, *8* (1), 29–34.

(12) Plank, C.; Zatloukal, K.; Cotton, M.; Mechtler, K.; Wagner, E. Gene transfer into hepatocytes using asialoglycoprotein receptor mediated endocytosis of DNA complexed with an artificial tetra-antennary galactose ligand. *Bioconjugate Chem.* **1992**, *3* (6), 533–539.

(13) Riviere, K.; Huang, Z.; Jerger, K.; Macaraeg, N.; Szoka, F. C. Antitumor effect of folate-targeted liposomal doxorubicin in KB tumor-bearing mice after intravenous administration. *J. Drug Targeting* **2010**, available online Mar 30 DOI: 10.3109/10611861003733953.

(14) Huckett, B.; Ariatti, M.; Hawtrey, A. O. Evidence for targeted gene transfer by receptor-mediated endocytosis. Stable expression following insulin-directed entry of NEO into HepG2 cells. *Biochem. Pharmacol.* **1990**, *40* (2), 253–263.

(15) Rosenkranz, A. A.; Yachmenev, S. V.; Jans, D. A.; Serebryakova, N. V.; Murav'ev, V. I.; Peters, R.; Sobolev, A. S. Receptor-mediated endocytosis and nuclear transport of a transfecting DNA construct. *Exp. Cell Res.* **1992**, *199* (2), 323–329.

(16) Li, Y.; Ogris, M.; Wagner, E.; Pelisek, J.; Rüffer, M. Nanoparticles bearing polyethyleneglycol-coupled transferrin as gene carriers: preparation and in vitro evaluation. *Int. J. Pharm.* **2003**, *259* (1−2), 93–101.

(17) Huang, R. Q.; Qu, Y. H.; Ke, W. L.; Zhu, J. H.; Pei, Y. Y.; Jiang, C. Efficient gene delivery targeted to the brain using a transferrin-conjugated polyethyleneglycol-modified polyamidoamine dendrimer. *FASEB J.* **2007**, *21* (4), 1117–1125.

(18) Lee, J. H.; Engler, J. A.; Collawn, J. F.; Moore, B. A. Receptor mediated uptake of peptides that bind the human transferrin receptor. *Eur. J. Biochem.* **2001**, *268* (7), 2004–2012.

(19) Oh, S.; Kim, B. J.; Singh, N. P.; Lai, H.; Sasaki, T. Synthesis and anti-cancer activity of covalent conjugates of artemisinin and a transferrin-receptor targeting peptide. *Cancer Lett.* **2009**, *274* (1), 33–9.

tion of a dendrimer−drug (i.e., host−guest) supramolecular assembly.[22] It has been reported that the interior region of dendrimers can be employed to encapsulate hydrophobic antitumor drugs.[22−24] The nanometer structure and simple modification make polyamidoamine dendrimer (PAMAM) a kind of ideal vector for passive and active tumor-targeting studies. Thus, the enrichment of antitumor drugs in tumor tissues can be realized with PAMAM as the carrier.

In addition, it has been reported that PAMAM showed pH-sensitivity itself.[25] The size and structure of PAMAM could change along with pH. When pH value decreased, the conformation of PAMAM changed from a "dense core" (high pH) to a "dense shell" (low pH).[25] As the pH in the tumor microenvironment is relatively low, the encapsulated drugs within PAMAM might be released quickly in tumor tissues.

Herein, we introduce the development of doxorubicin (DOX)-loaded T7-modified PEGylated PAMAM dendrimers (PAMAM-PEG-T7/DOX) for cancer therapy. The conjugation of T7 to PAMAM was achieved by chemically coupling the cysteine-modified T7 to maleimide-PEG-PAMAM which subsequently encapsulates DOX. The tumor-targeting efficiency of PAMAM-PEG-T7/DOX nanoparticles (NPs) was evaluated in vitro and in vivo. Furthermore, the in vivo antitumor effect of PAMAM-PEG-T7/DOX NPs was explored.

## Materials and Methods

**Chemicals.** DOX was provided by Huafeng United Technology (Beijing, China). PAMAM G5 dendrimer [77.35 $\mu$g/$\mu$L in methyl alcohol, containing 128 surface primary amino groups (MW 28 826)], TES (*N*-tris-hydroxymethyl-methyl-2-aminoethanesulfonic acid), and holo-Tf were obtained from a commercially prepared collection from Sigma-Aldrich (St. Louis, MO). T7 with a cysteine on the N-terminal (cys-T7) was synthesized by Chinese Peptide Company (Hangzhou, China). α-Maleimidyl-*ω*-*N*-hydroxysuccinimidyl poly(ethylene glycol) (NHS-PEG-Mal, MW 3400) was obtained from Nektar Therapeutics (Huntsville, AL).

**Cells.** Human hepatocellular carcinoma cells (Bel-7402) were purchased from Cell Bank, Chinese Academy of Sciences (Shanghai, China). Briefly, Bel-7402 cells were maintained in RPMI medium 1640 (Invitrogen Corporation) supplemented with 10% heat-inactivated fetal calf serum (FCS), 100 U/mL penicillin, and 100 $\mu$g/mL streptomycin and cultured at 37 °C under a humidified atmosphere containing 5% $CO_2$.

**Mice.** BALB/c nude mice, male, age 4−5 weeks, body weight 20−25 g, were purchased from the Department of Experimental Animals, Fudan University, and maintained under standard housing conditions. All animal experiments were carried out in accordance with guidelines evaluated and approved by the ethics committee of Fudan University. For construction of xenograft model Bel-7402, $3 \times 10^6$ Bel-7402 cells in a volume of 100 $\mu$L of serum free RPMI were inoculated subcutaneously into the right flank region of mice.

**Synthesis of PAMAM Derivatives.** PAMAM G5 was reacted with MAL-$PEG_{3400}$-NHS (PBS 8.0) at the ratio 1:10 (mol/mol) for 2 h at room temperature. The primary amino groups on the surface of PAMAM were specially reacted with the terminal NHS groups of the bifunctional PEG derivative. The resulting conjugate, PAMAM-PEG, was purified by ultrafiltration using a 5 kDa molecular weight cutoff membrane to remove unreacted PEG, and the buffer was exchanged into PBS (pH 7.0). Then PAMAM-PEG was further reacted with cys-T7 at the ratio of 1:5 (mol/mol) and stirred at room temperature for 24 h to synthesize PAMAM-PEG-T7.

PAMAM-PEG-Tf was synthesized as described previously with a little modification.[17] PAMAM-PEG was reacted with thiolated Tf, 1:5 (mol/mol) in PBS (pH 7.0) for 24 h at room temperature.

**Characterization of PAMAM-PEG-T7.** Small angle X-ray scattering (SAXS) characterization was conducted to probe the surface structure of the vector PAMAM-PEG-T7 in pH 7.4 and 5.5. PAMAM-PEG-T7 in pH 7.4 or 5.5 was directly introduced into a capillary glass tube and sealed with heating for SAXS measurements.

**Encapsulation of DOX by PAMAM Derivatives.** PAMAM G5 was mixed with DOX solution (1 mg/mL) at ratios of 1:6, 1:8, 1:12, and 1:40 (mol/mol) in methanol and agitated at room temperature for 12 h. The above product was transferred to 10 mM pH 7.4 TES buffer after rotary evaporation. The unincorporated DOX was removed by ultrafiltration through a membrane (cutoff = 3 kDa) to purify the complex and get encapsulation efficiency. For encapsulation by PAMAM derivatives, the method was same as that of entrapment by PAMAM G5. Freshly prepared NPs were used in the experiments that follow.

**Characterization of PAMAM-PEG-T7/DOX NPs.** The morphologic study of PAMAM-PEG-T7/DOX NPs was assessed with the use of bioscope atomic force microscopy (Veeco Instruments Inc.). The mean diameter of PAMAM-

(20) Esfand, R.; Tomalia, D. A. Poly(amidoamine) (PAMAM) dendrimers: from biomimicry to drug delivery and biomedical applications. *Drug Discovery Today* **2001**, *6* (8), 427–436.
(21) Liu, M.; Fréchet, J. M. Designing dendrimers for drug delivery. *Pharm. Sci. Technol. Today* **1999**, *2* (10), 393–401.
(22) Morgan, M. T.; Nakanishi, Y.; Kroll, D. J.; Griset, A. P.; Carnahan, M. A.; Wathier, M.; Oberlies, N. H.; Manikumar, G.; Wani, M. C.; Grinstaff, M. W. Dendrimer-encapsulated camptothecins: increased solubility, cellular uptake, and cellular retention affords enhanced anticancer activity in vitro. *Cancer Res.* **2006**, *66* (24), 11913–11921.
(23) Ke, W.; Zhao, Y.; Huang, R.; Jiang, C.; Pei, Y. Enhanced oral bioavailability of doxorubicin in a dendrimer drug delivery system. *J. Pharm. Sci.* **2008**, *97* (6), 2208–2216.
(24) Kojima, C.; Kono, K.; Maruyama, K.; Takagishi, T. Synthesis of polyamidoamine dendrimers having poly(ethylene glycol) grafts and their ability to encapsulate anticancer drugs. *Bioconjugate Chem.* **2000**, *11* (6), 910–917.
(25) Liu, Y.; Bryantsev, V. S.; Diallo, M. S.; Goddard Iii, W. A. PAMAM Dendrimers Undergo pH Responsive Conformational Changes without Swelling. *J. Am. Chem. Soc.* **2009**, *131* (8), 2798–2799.

PEG-T7/DOX NPs was measured by dynamic light scattering using a zeta potential/particle sizer NicompTM 380 ZLS (PSS Nicomp Particle Size System).

**In Vitro Release Studies.** In vitro DOX release from the PAMAM-PEG-T7/DOX NPs was performed using the dialysis method. A 450 $\mu$L solution of the formulation was placed in the dialysis bag (MWCO 1000 Da), hermetically clamped, and immediately suspended in 200 mL 0.01 M acetate buffer pH 5.5 or in 0.01 M TES pH 7.4. The absorbance of DOX released at various times was measured on a microplate fluorometer (Perkin-Elmer) at Ex/Em 537/584 nm. The volume of the recipient compartment was maintained by replenishing 1 mL of sink solution after each withdrawal of 1 mL aliquot.

**Characterization of Drug Encapsulation.** The mechanism of DOX encapsulation was analyzed by differential scanning calorimetry (DSC). The physical state of DOX loaded in PAMAM-PEG-T7/DOX NPs was investigated using DSC (NETISCH-Geratebau GmbH, Germany). Freeze-dried NPs were subjected to DSC with native DOX as control. For DSC, a heating rate of 10 °C/min was used.

**Cellular Uptake.** Bel-7402 cells were seeded at a density of $5 \times 10^4$ cells/well in 24-well plates (Corning-Coaster, Tokyo, Japan), incubated for 48 h, and checked under the microscope for confluency and morphology. Then cells were incubated with DOX, PAMAM-PEG/DOX, and PAMAM-PEG-T7/DOX (DOX 4.35 $\mu$g and PAMAM 36 $\mu$g/well) in the presence of serum free medium for 30 min at 37 °C. To confirm the promotion of Tf in PAMAM-PEG-T7/DOX NPs internalization into cells, groups with Tf (25 $\mu$M) were added. PAMAM-PEG-Tf/DOX was used as control. After 30 min incubation, cells were washed with Hanks' balanced salt solution and then visualized and photographed under an IX2-RFACA fluorescent microscope (Olympus, Osaka, Japan).

**Cytotoxicity.** Bel-7402 cells were seeded at a density of $5 \times 10^3$ cells/well in 96-well plates (Corning-Coaster, Tokyo, Japan) and incubated for 24 h. Then cells were incubated with PAMAM-PEG-T7/DOX NPs at varying concentrations for 48 h at 37 °C. PAMAM-PEG-T7/DOX NPs in the presence of free Tf (25 $\mu$M) were set to study whether the cytotoxicity could be enhanced by addition of free Tf. Free DOX and PAMAM-PEG/DOX were used as control. After 48 h incubation, surviving cells were evaluated using MTT Cell Proliferation Assay.

**Ex Vivo Imaging Analysis.** A human hepatocellular carcinoma xenograft model was established in BALB/c mice by subcutaneous injection of $3 \times 10^6$ Bel-7402 cells. PAMAM-PEG/DOX and PAMAM-PEG-T7/DOX NPs were injected into the tail vein of mice bearing Bel-7402 tumors (PAMAM 330 $\mu$g and DOX 40 $\mu$g/mouse), respectively. Free DOX (DOX 100 $\mu$g/mouse) was used as a control. Four hours later, the nude mice were sacrificed, and tumors and normal organs collected from the animals and visualized by using a CRi in vivo imaging system (CRi, Woburn, MA).

**Pharmacokinetic and Biodistribution Studies.** When the subcutaneous hepatocellular carcinoma xenografts were grown to a palpable size (90−130 $mm^2$), the experiment was initiated. Mice bearing Bel-7402 tumors were weighed, marked, and divided into three groups (each group including 30 mice with 6 mice per time point). Free DOX, PAMAM-PEG/DOX NPs, or PAMAM-PEG-T7/DOX NPs (2 mg DOX/kg body weight) were administered intravenously. Two groups with healthy mice were added as control for the treatment of PAMAM-PEG-T7/DOX NPs and PAMAM-PEG/DOX NPs. The blood samples were collected from the retro-orbital plexus of the rat eye at 5 min, 15 min, 30 min, 60 min, and 4 h. In every time point, after the collection of blood, mice were sacrificed, and organs and tumors were carefully removed and stored under frozen conditions.

In each case, blood was centrifuged at 3000 rpm for 10 min to separate red blood cells (RBCs) and serum and the supernatant (serum) was collected with the help of a micropipet. Daunomycin (DAM) (4 $\mu$g/mL × 30 $\mu$L) as internal standard was added to the samples (200 $\mu$L). The contents were vortexed for 10 s, and 2 mL of chloroform/methanol (4:1) was added. The drug was extracted by vortexing for 2 min and centrifuged at 3000 rpm for 10 min. The underlayer was transferred to another vial and evaporated to dryness at 40 °C. The dried residue was redissolved with 100 $\mu$L of mobile phase and analyzed for DOX content.

Tissue samples were taken out, weighed, and homogenized to separate the tissues. Then the contents were treated with 30 $\mu$L of DAM and vortexed for 10 s, and 2 mL of chloroform/methanol (4:1) was added. The drug was extracted for 2 min and centrifuged at 3000 rpm for 10 min. The underlayer was transferred to another centrifuge tube and evaporated to dryness at 40 °C. The dried residue was redissolved with 100 $\mu$L of mobile phase and analyzed for drug content.

Estimation of DOX in serum and various tissues (liver, spleen, and kidney and tumor homogenate) was performed by HPLC (Agilent) method as previously reported[26] with minor modifications. The flow rate was maintained at 1.0 mL/min, and the run time was adjusted to 12 min.

The results were expressed as mean ± SD, and the statistical analysis was done by analysis of variance (ANOVA). A probability level of $p < 0.05$ was considered to be significant.

**In Vivo Antitumor Effect.** Mice were randomly distributed to the experimental groups (6 mice per group). When the subcutaneous hepatocellular carcinoma xenografts were grown to a palpable size (200−300 $mm^3$), formulations were administered intravenously to treat the tumors. Mice were treated with PAMAM-PEG/DOX NPs or PAMAM-PEG-T7/DOX (2 mg DOX/kg body weight) three times on days 0, 7, and 14. For clinical DOX, mice were treated with 5 mg DOX/kg body weight three times. The treatment ended on day 16. On day 16, tumors were excised and photographed. Changes of body weight were registered to evaluate the NPs' toxicity. The tumor growth inhibitory effect

(26) Reddy, L. H.; Meda, N.; Murthy, R. R. Rapid and sensitive HPLC method for the estimation of doxorubicin in dog blood--the silver nitrate artifact. *Acta Pharm.* **2005**, *55* (1), 81–91.

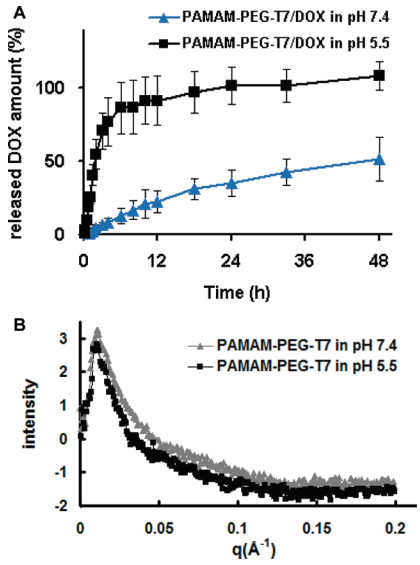


***Figure 1.*** In vitro release and characterization of PAMAM-PEG-T7/DOX NPs. (A) In vitro drug release studies. PAMAM-PEG-T7/DOX NP release curves were investigated in pH 5.5 (■) and 7.4 (▲). (B) SAXS profiles of PAMAM-PEG-T7 in pH 5.5 (■) and 7.4 (▲).

of various treatments was controlled within 3 weeks following the treatments using a digital caliper. Tumor volume was calculated using the following formula: $V = a^2 \times b \times \pi/6$ (where $a$ and $b$ mean the shortest and the longest diameter, respectively, of a given tumor).[27] Mean values and standard deviations were calculated.

**Statistical Analysis.** All of the quantitative measurements were collected in quadruplicate, and the experiments were repeated four times. The data are expressed as mean ± SE. Statistical analysis was performed by one-way ANOVA and was followed by Bonferroni's post-test using Stata software (version 7.0).

## Results

**Characterization of PAMAM-PEG-T7/DOX NPs.** The interior region of PAMAM G5 could be effectively utilized to carry hydrophobic drugs and control their release behavior by hydrophobic interaction. Entrapment efficiency of DOX by PAMAM G5 was measured at different feed ratios (Supporting Information Figure S1). NPs at a feed ratio 1:6 were used in the following experiments. The DOX release from PAMAM-PEG-T7 was investigated at pH 7.4 and 5.5 (Figure 1A). A slow release was observed over 48 h in pH 7.4 (51.55% at 48 h). At pH 5.5, DOX was completely released much before 48 h.

SAXS studies were performed to characterize the surface structure of PAMAM-PEG-T7 (Figure 1B). In the SAXS diagram, the higher scattering intensity corresponds to a higher degree of the compact. The scattering intensity of PAMAM-PEG-T7 in pH 7.4 was slightly higher than that in pH 5.5 (Figure 1B).

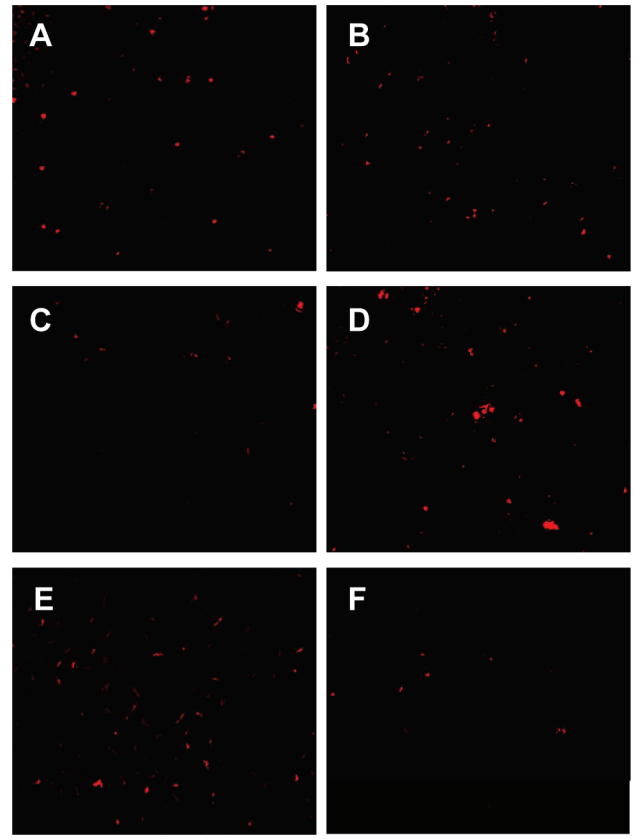


***Figure 2.*** Cellular uptake of PAMAM-PEG-T7/DOX NPs (C, E) and PAMAM-PEG-Tf/DOX NPs (D, F) examined by fluorescent microscopy after 30 min incubation: (A) DOX, (B) PAMAM/DOX, (C) PAMAM-PEG-T7/DOX NPs without Tf, (D) PAMAM-PEG-Tf/DOX NPs without Tf, (E) PAMAM-PEG-T7/DOX NPs with Tf, and (F) PAMAM-PEG-Tf/DOX NPs with Tf. Red: DOX. Original magnification: ×100.

An atomic force microscopy image exhibiting the spherical morphology and similar diameter of PAMAM-PEG-T7/DOX NPs is shown in Supporting Information Figure S2. The mean diameter of PAMAM-PEG-T7/DOX NPs was 10 nm (Supporting Information Figure S3).

DSC thermograms of free DOX showed one endotherm appearing at about 175 °C (Supporting Information Figure S4). The endotherm corresponds to the melting peak of DOX. The thermogram of blank vector PAMAM-PEG-T7 showed no endotherm near the melting peak of DOX (Supporting Information Figure S4). However, the endotherm corresponding to DOX melting was not observed in thermograms of PAMAM-PEG-T7/DOX and PAMAM/DOX (Supporting Information Figure S4). It indicates that phase transformation occurred and DOX existed in amorphous form in PAMAM-PEG-T7/DOX NPs. In addition, the peak appearing at about 54 °C fits the melting point of PEG 3500 (Supporting Information Figure S4A and B). PAMAM G5 possesses a

(27) Tomayko, M. M.; Reynolds, C. P. Determination of subcutaneous tumor size in athymic (nude) mice. *Cancer Chemother. Pharmacol.* **1989**, *24* (3), 148–154.

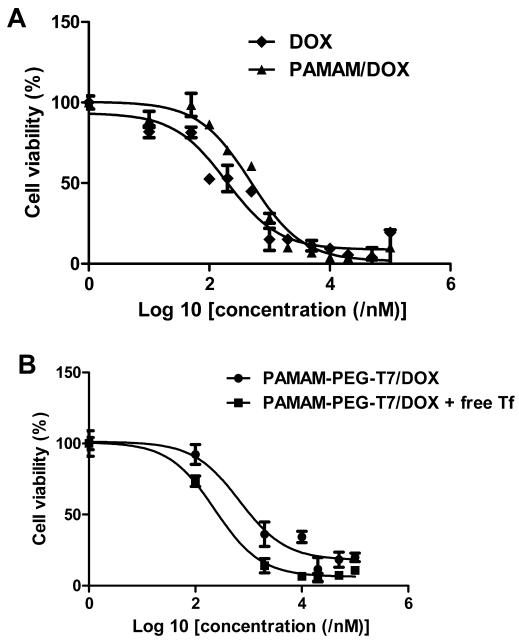


***Figure 3.*** Cytotoxicity of free DOX, PAMAM/DOX, and PAMAM-PEG-T7/DOX NPs to Bel-7402 cells. Cell viability was expressed as the percentage of the untreated control cells. (A) Bel-7402 cells were incubated in 96-well plates and treated with free DOX (◆) and PAMAM/DOX (▲). (B) Bel-7402 cells were treated with PAMAM-PEG-T7/DOX with Tf (■) and PAMAM-PEG-T7/DOX without Tf (●). The curve was fit with GraphPad Prism version 5.0.

melting temperature of approximately 30 °C (Supporting Information Figure S4A and B).

**Cellular Uptake.** The cellular uptake of DOX-loaded NPs was investigated using fluorescence microscopy in Bel-7402 cells (Figure 2). Tf at a concentration of 25 $\mu$M was used to represent endogenous Tf in the blood. As expected, the fluorescence intensity increased dramatically when encapsulated in PAMAM against free DOX (Figure 2A). Second, the cellular fluorescence intensity of PAMAM-PEG-T7/DOX NPs co-treated with free Tf was superior to that of PAMAM-PEG-T7/DOX NPs without Tf. The cellular uptake of PAMAM-PEG-Tf/DOX NPs co-treated with free Tf was inferior to that of PAMAM-PEG-Tf/DOX NPs without Tf. PAMAM-PEG-T7/DOX NPs in the presence of free Tf showed the highest cellular uptake.

**Cytotoxicity.** Cell viability after incubation with the PAMAM-PEG-T7/DOX NPs was examined to evaluate the in vitro antitumor effect (Figure 3). The cytotoxicity of PAMAM-PEG/DOX NPs and free DOX was also measured as control. PAMAM/DOX NPs exhibited higher cytotoxicity than free DOX. In addition, the toxicity of PAMAM-PEG-T7 without Tf was lower than that of PAMAM-PEG-T7/DOX NPs with Tf.

The $IC_{50}$ values for PAMAM-PEG-T7/DOX with and without Tf and PAMAM/DOX NPs and free DOX are shown in Table 1. PAMAM-PEG-T7/DOX exhibited higher toxicity toward tumor cells in the presence of Tf than that in the absence of Tf. The $IC_{50}$ value for PAMAM-PEG-T7/DOX was pretty close to that for free DOX.

***Table 1.*** $IC_{50}$ of Free DOX and DOX-Encapsulated NPs for Bel-7402 Cells

| formulation | $IC_{50}$ (nM) |
|---|---|
| free DOX | 191.5 ± 7.0 |
| PAMAM/DOX | 483.4 ± 4.0 |
| PAMAM-PEG-T7/DOX − Tf | 676.7 ± 7.1 |
| PAMAM-PEG-T7/DOX + Tf | 231.5 ± 3.0 |

**Pharmacokinetic Studies.** Pharmacokinetic was studied to investigate whether it significantly differs between PAMAM-PEG-T7/DOX NPs, PAMAM-PEG/DOX, and free DOX. After administration, DOX was distributed and eliminated very quickly (Figure 4). The DOX concentration in blood reached equilibrium basically within 30 min. However, there is no evident distinction between free DOX and PAMAM-PEG/DOX NPs and PAMAM-PEG-T7 NPs, and between healthy mice and mice bearing Bel-7402 tumors (Figure 4). Also, no significant distinction is shown between the pharmacokinetic parameters of free drug DOX and formulations (data not shown).

**Ex Vivo Imaging Analysis.** Mice bearing Bel-7402 tumors were injected with either PAMAM-PEG-T7/DOX NPs or PAMAM-PEG/DOX NPs, and free DOX at high dose as positive control or saline as negative control. Ex vivo fluorescent images were taken at 4 h after injection. As shown in Figure 5, DOX obviously accumulated in the tumor of the mouse treated with PAMAM-PEG-T7/DOX NPs

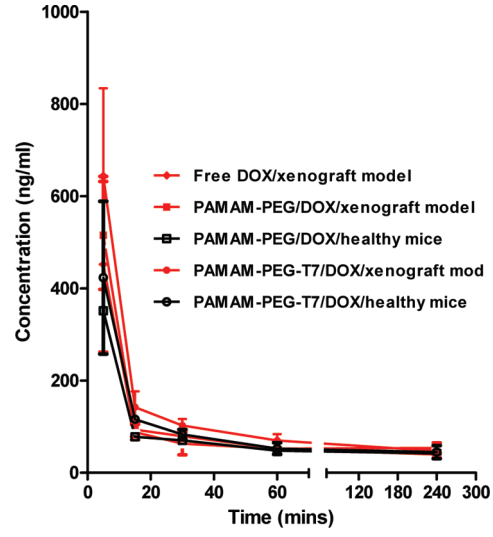


***Figure 4.*** Plasma concentration profiles of free DOX, PAMAM-PEG/DOX NPs, and PAMAM-PEG-T7/DOX NPs. Mice bearing Bel-7402 tumors received one intravenous injection of either free DOX (◆), PAMAM-PEG/DOX (■), or PAMAM-PEG-T7/DOX (●) at a dose of 2 mg DOX/kg. Healthy mice treated with one intravenous injection of PAMAM-PEG/DOX NPs (□) or PAMAM-PEG-T7/DOX NPs (○) were used as controls. Each value represents the mean ± SD of six experiments.

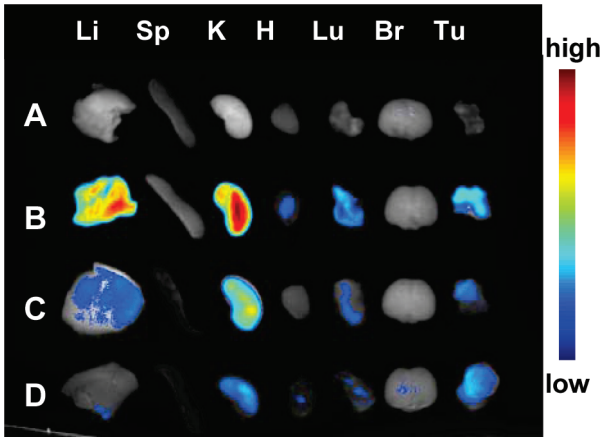


***Figure 5.*** Fluorescence images showing qualitative biodistribution of DOX in mice bearing Bel-7402 tumors at 4 h after injection of either free DOX (5 mg DOX/kg) (B), PAMAM-PEG/DOX (2 mg DOX/kg) (C), or PAMAM-PEG-T7/DOX (2 mg DOX/kg) (D). The saline treatment was used as a control (A). H, Li, Sp, Lu, K, Br, and Tu indicate heart, liver, spleen, lung, kidney, brain, and tumor, respectively.

(Figure 5). Comparing with PAMAM-PEG/DOX NPs and high dose free DOX, the fluorescence of DOX in the mouse treated with PAMAM-PEG-T7/DOX NPs was almost absent in the liver, kidney, and lung (Figure 5).

**Biodistribution Studies.** The DOX concentration in the tumor of mice treated with PAMAM-PEG-T7/DOX was significantly increased compared with that of free DOX ($P < 0.001$) and PAMAM-PEG/DOX ($P < 0.05$) (Figure 6A). In addition, for mice bearing Bel-7402 tumors, the concentration of PAMAM-PEG-T7/DOX in liver, kidney, heart, spleen, and lung was lower than that of free DOX and PAMAM-PEG/DOX (Figure 6B).

**In Vivo Antitumor Effect.** Mice bearing Bel-7402 tumors with a tumor size of 200−300 $mm^3$ received the treatment. The inhibition of tumor growth was more evident in the groups treated with PAMAM-PEG-T7/DOX NPs (2 mg/kg) and DOX in high dose (5 mg/kg) than in those treated with PAMAM-PEG/DOX (2 mg/kg) and saline (Figure 7A and B). When the treatment ended, tumor growth of the mice treated with PAMAM-PEG-T7/DOX NPs was inhibited by 33.0%, 51.1%, and 71.4%, respectively (data not shown), comparing with that treated with DOX, PAMAM-PEG/DOX NPs, and saline (Figure 7A). However, in the free DOX group, obvious weight loss was observed, especially at 2 days after each administration. The results showed that low-dose PAMAM-PEG-T7/DOX NPs possessed an antitumor effect comparable to that of high-dose free DOX without significant side effects.

## Discussion

The high drug accumulation in the tumor and the low side effects can be achieved by the tumor-targeting delivery systems which are designed based on the different pathological features between tumor and normal tissues.

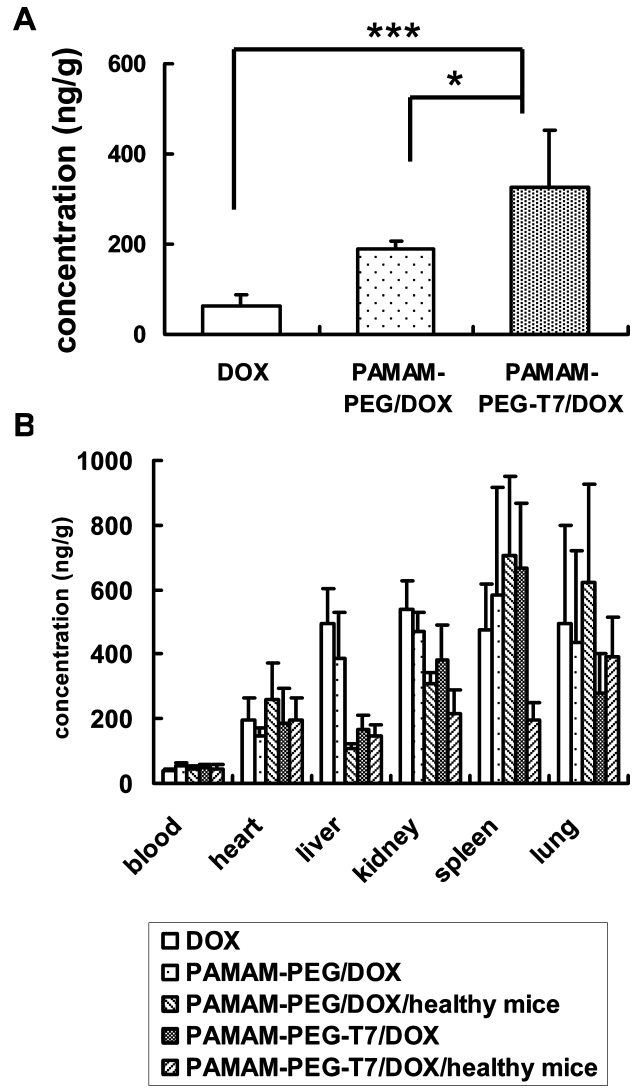


***Figure 6.*** Tumor (A) and normal organ (B) accumulation of DOX in mice bearing Bel-7402 tumors at 4 h postinjection of either free DOX, PAMAM-PEG/DOX NPs, or PAMAM-PEG-T7/DOX NPs at a dose of 2 mg DOX/kg. Healthy mice treated with one intravenous injection of either PAMAM-PEG/DOX NPs or PAMAM-PEG-T7/DOX NPs were used as controls. Each value represents the mean ± SD of six experiments. (*** $P < 0.001$; * $P < 0.05$).

In this study, PAMAM-PEG-T7 was successfully synthesized and used to encapsulate DOX to construct a tumor-targeting drug delivery system, PAMAM-PEG-T7/DOX NPs. These PAMAM-PEG-T7/DOX NPs could accumulate efficiently in the tumor due to their nanoscaled size, TfR-targeting properties, and pH-sensitive release of drug.

Most tumors grown subcutaneously in the dorsal chamber have a vascular pore cutoff size ranging between 380 and 760 nm.[28,29] NPs with a size of less than 380 nm can directly enter the tumor by extravasating into tumor vasculature.[4] The size of PAMAM-PEG-T7/DOX NPs prepared in this work was approximately 10 nm (Supporting Information Figures S2 and S3). Thus, PAMAM-PEG-T7/DOX NPs could be entrapped in tumor tissues via the EPR effect. The result

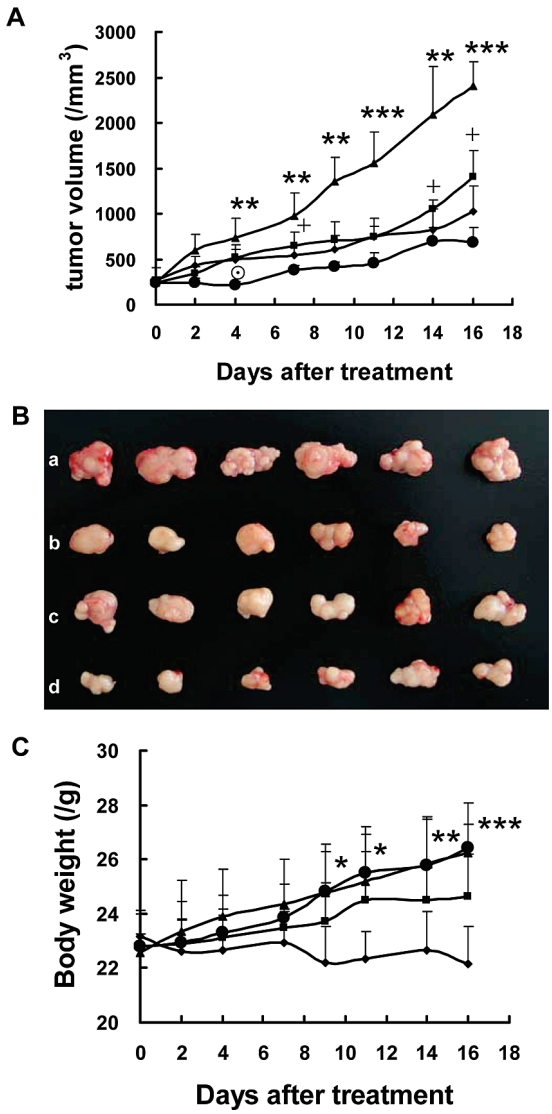


***Figure 7.*** (A) Xenograft tumor treatment measurements in mice. Mice bearing Bel-7402 tumors received three intravenous injections on days 0, 7, and 14 of free DOX (5 mg/kg) (◆), PAMAM-PEG/DOX NPs (2 mg DOX/kg) (■), or PAMAM-PEG-T7/DOX NPs (2 mg DOX/kg) (●) in different groups as shown. The saline treatment (▲) was used as a control (***, **, and * indicate $P < 0.001$, 0.01, and 0.05 versus PAMAM-PEG-T7/DOX NPs or control; + indicates $P < 0.05$ versus PAMAM-PEG-T7/DOX NPs or PAMAM-PEG/DOX NPs; ⊙ indicates $P < 0.05$ versus PAMAM-PEG-T7/DOX NPs or DOX). (B) Excised tumors from mice bearing Bel-7402 tumors at day 16 after treatments of free DOX (b), PAMAM-PEG/DOX (c), or PAMAM-PEG-T7/DOX (d) in different groups as shown. The saline treatment was used as a control (a). Tumors excised were stored at −80 °C and imaged together with all other groups at the end of the study. (C) Body weight change in mice over 16 days after mice bearing Bel-7402 tumors treated with free DOX (5 mg/kg) (◆), PAMAM-PEG/DOX (2 mg DOX/kg) (■), or PAMAM-PEG-T7/DOX (2 mg DOX/kg) (●) on days 0, 7, and 14. Each value represents the mean ± SD of six experiments (***, **, and * indicate $P < 0.001$, 0.01, and 0.05 versus DOX or control).

shown in Figure 6 demonstrated that the accumulation of PAMAM-PEG/DOX NPs in the tumor was about 5.5-fold higher than that of free DOX. It further indicated that the accumulation and retention of drugs would be enhanced in tumor tissues compared to those in normal tissues due to the well-known EPR effect.

From the release behavior of DOX from PAMAM-PEG-T7 in normal conditions, the hydrophobic interaction between DOX and the interior region of PAMAM G5 was strong enough to retain the drug; DOX was released from PAMAM-PEG-T7/DOX NPs slowly (Figure 1A). This is inconsistent with the release characteristics of DOX from M-PEG (2000)-PAMAM G3 or G4.[24] The reason might reside in the difference of the generation of PAMAM and the PEGylation degree. Furthermore, PAMAM goes through a pH-induced conformational change from a "dense core" (high pH) to a "dense shell" (low pH),[25] suggesting that encapsulation and release of drugs can be controlled using pH as the trigger. The pH dependence of the structure and size of dendrimers is a critical issue for utilization as drug delivery vehicles in physiological environments (pH = 5−7.4). Previous work exhibited dramatic changes in the conformations, where it was shown that the high pH form has a "dense core" (with a maximum density at the dendrimer core and uniform void spacings), whereas ion pairing at low pH leads to a "dense shell" (with maximum density at the dendrimer periphery but nonuniform void spacings).[25] On the other hand, the effect of pH on the size of dendrimers was very little. Previous small angle neutron scattering (SANS) experiments on a G8 polyamidoamine (PAMAM) showed a 2% increase of the radius of gyration from pH 10.1 to 4.7.[30] The insensitivity of size to the variation of pH was confirmed in the recent SANS experiment on a G4 PAMAM.[31] Therefore, the variation of the scattering intensities was very tiny but not negligible (Figure 1B). The change of the intensities may result from the conformation changes, which finally leads to the drug release. This rationale was validated in this work, where the release of DOX was much faster at pH 5.5 (Figure 1A).

The EPR effect is the most important pathological basis for designing tumor-targeting drug delivery systems via both passive and active mechanisms. Ligand-modified active-targeting delivery systems also need to extravasate in tumor

(28) Yuan, F.; Dellian, M.; Fukumura, D.; Leunig, M.; Berk, D. A.; Torchilin, V. P.; Jain, R. K. Vascular permeability in a human tumor xenograft: molecular size dependence and cutoff size. *Cancer Res.* **1995**, *55* (17), 3752–3756.

(29) Hobbs, S. K.; Monsky, W. L.; Yuan, F.; Roberts, W. G.; Griffith, L.; Torchilin, V. P.; Jain, R. K. Regulation of transport pathways in tumor vessels: role of tumor type and microenvironment. *Proc. Natl. Acad. Sci. U.S.A.* **1998**, *95* (8), 4607–4612.

(30) Nisato, G.; Ivkov, R.; Amis, E. J. Size Invariance of Polyelectrolyte Dendrimers. *Macromolecules* **2000**, *33* (11), 4172–4176.

(31) Chen, W. R.; Porcar, L.; Liu, Y.; Butler, P. D.; Magid, L. J. Small Angle Neutron Scattering Studies of the Counterion Effects on the Molecular Conformation and Structure of Charged G4 PAMAM Dendrimers in Aqueous Solutions. *Macromolecules* **2007**, *40* (16), 5887–5898.

vasculature via EPR effect to reach tumor cells initially. It has been reported that the nanoscaled delivery systems are entrapped in tumor tissues rapidly through the EPR effect after intravenous administration.[32] However, different systems have different elimination rates. For example, *N*-(2-hydroxypropyl)-methacrylamide (HPMA) NPs were mostly cleared by the tumor within 10 min,[30] while more than 90% of siRNA-loaded protamine-based NPs disappeared in plasma and 70−80% accumulated in the tumor in the early 4 h.[33] In this study, PAMAM-PEG/DOX NPs almost disappeared in plasma at 20 min postinjection (Figure 4). According to the biodistribution studies (Figure 6), the accumulation of PAMAM-PEG/DOX NPs in the tumor was similar to that of PAMAM-PEG-T7/DOX NPs, and both were obviously higher than that of free DOX at 1 h after the treatment (data not shown). Four hours later, the result showed apparently higher accumulation of PAMAM-PEG-T7/DOX NPs in the tumor than that of PAMAM-PEG/DOX NPs. These results demonstrated that early phase tumor accumulation of NPs might be mainly through the EPR effect, which had been suggested previously.[33]

There exist two tumor-targeting strategies, including (1) passive targeting delivery mainly through the EPR effect of tumor vessels and (2) active targeting delivery by receptor-mediated endocytosis. The receptor-mediated endocytosis involves in the relatively higher expression of receptors in tumor cells than that in normal cells. TfR was expressed at a high level (150 000−1 000 000 per cell) on the surface of tumor cells.[34,35] Therefore, Tf was widely applied as a carrier or targeting ligand for active targeting delivery of anticancer agents, proteins, and genes to malignant cells that overexpress TfR.[36] However, most of the encouraging results were obtained in vitro. The in vivo application of Tf-modified drug delivery systems was limited probably due to intense competition of endogenous Tf.

As for T7, the binding site of T7 to the human TfR was identified to be different from that of Tf to TfR.[18,19] To further improve the tumor-targeting efficiency, T7 was used in this study to trigger the receptor-mediated internalization of PAMAM-PEG-T7/DOX NPs in the tumor. As shown in Figure 2, the cellular fluorescence intensity of PAMAM-PEG-T7/DOX NPs co-treated with free Tf was superior to that without Tf. In contrast, the cellular uptake of PAMAM-PEG-Tf/DOX NPs co-treated with free Tf was inferior to that without Tf. It suggested that the addition of free Tf at a plasma concentration of 25 $\mu$M inhibited the cellular uptake of PAMAM-PEG-Tf/DOX but promoted the internalization of PAMAM-PEG-T7/DOX NPs. These results are in accordance with previous reports, which presumed that the binding site of T7 on TfR was among the cavities that do not overlap with the binding site of Tf.[18,19] And some of these cavities were used for binding to regulatory proteins such as hereditary hemochromatosis protein HFE.[37,38] Correspondingly, PAMAM-PEG-T7/DOX with Tf exhibited the highest cytotoxicity (Figure 6). Similar results were observed that the HPMA copolymer-bound DOX targeted with Tf showed an approximately 2.5-fold higher cytotoxic effect than the nontargeted counterpart.[39] However, the Tf-modified conjugate was less effective in vivo and cured only one out of seven experimental mice.[39] Thus, it implied that PAMAM-PEG-T7/DOX NPs can be efficiently internalized into tumor cells with the help of endogenous Tf. The cellular uptake of free DOX is through simple diffusion. However, the uptake of PAMAM-PEG-T7/DOX was mainly through receptor-mediated endocytosis. The rate of simple diffusion is higher than that of receptor-mediated endocytosis. Therefore, the PAMAM-PEG-T7 exhibited higher $IC_{50}$ than that of free DOX (Table 1).

In addition, the enhanced distribution in the tumor may be attributed to the TfR-mediated transfer, while that of PAMAM-PEG/DOX NPs could be interpreted as a passive targeting mechanism through the EPR effect.[4] However, the accumulation of PAMAM-PEG-T7/DOX NPs in liver and kidney was apparently reduced compared with that of PAMAM-PEG/DOX NPs (Figures 5 and 6). Most free DOX distributed in the kidney and liver after administration and cleared quickly. Although renal and hepatic clearance of DOX was reduced, PAMAM-PEG-T7 did not show significant difference in in vivo resident time from free DOX because of its efficient and fast accumulation in tumor (Figure 4). The results indicated that T7 played a critical role in the distribution of NPs in the tumor and the tumor-targeting efficiency was enhanced significantly by T7. Correspondingly, PAMAM-PEG-T7/DOX NPs showed the most effec-

(32) Noguchi, Y.; Wu, J.; Duncan, R.; Strohalm, J.; Ulbrich, K.; Akaike, T.; Maeda, H. Early phase tumor accumulation of macromolecules: a great difference in clearance rate between tumor and normal tissues. *Jpn. J. Cancer Res.* **1998**, *89* (3), 307–14.

(33) Li, S. D.; Chono, S.; Huang, L. Efficient oncogene silencing and metastasis inhibition via systemic delivery of siRNA. *Mol. Ther.* **2008**, *16* (5), 942–946.

(34) Cazzola, M.; Bergamaschi, G.; Dezza, L.; Arosio, P. Manipulations of cellular iron metabolism for modulating normal and malignant cell proliferation: achievements and prospects. *Blood* **1990**, *75* (10), 1903–19.

(35) Kratz, F.; Beyer, U.; Roth, T.; Tarasova, N.; Collery, P.; Lechenault, F.; Cazabat, A.; Schumacher, P.; Unger, C.; Falken, U. Transferrin conjugates of doxorubicin: synthesis, characterization, cellular uptake, and in vitro efficacy. *J. Pharm. Sci.* **1998**, *87* (3), 338–346.

(36) Vyas, S. P.; Sihorkar, V. Endogenous carriers and ligands in non-immunogenic site-specific drug delivery. *Adv. Drug Delivery Rev.* **2000**, *43* (2−3), 101–164.

(37) Lebrón, J. A.; Bjorkman, P. J. The transferrin receptor binding site on HFE, the class I MHC-related protein mutated in hereditary hemochromatosis. *J. Mol. Biol.* **1999**, *289* (4), 1109–1118.

(38) Bennett, M. J.; Lebrón, J. A.; Bjorkman, P. J. Crystal structure of the hereditary haemochromatosis protein HFE complexed with transferrin receptor. *Nature* **2000**, *403* (6765), 46–53.

(39) Kovár, M.; Strohalm, J.; Ulbrich, K.; Ríhová, B. In vitro and in vivo effect of HPMA copolymer-bound doxorubicin targeted to transferrin receptor of B-cell lymphoma 38C13. *J. Drug Targeting* **2002**, *10* (1), 23–30.

tive antitumor effect (Figure 7). Two days after a course of treatment of PAMAM-PEG-T7/DOX NPs (2 mg/kg), tumor growth of mice was inhibited by 33.0%, 51.1%, and 71.4%, comparing to DOX (5 mg/kg), PAMAM-PEG/DOX NPs (2 mg/kg DOX), and saline, respectively. The results are in contrast with the work in Munns's group which showed that the Tf-DOX conjugate failed as a cytotoxic delivery system because it did not prevent toxicity to TfR-negative cells.[40] Likewise, mice treated with PAMAM-PEG-T7/DOX NPs had almost no weight loss, while that of mice administered with DOX was descending in the whole experimental process. The results are in good agreement with previous reports, where tumor-bearing animals treated with Tf and albumin-DOX conjugates had body weight loss of less than 10%.[41] Although the use of Tf as a ligand to mediate drug or gene tumor-targeting delivery has achieved enormous success,[39] the T7-modified drug delivery system may have better tumor-targeting efficiency.

(40) Munns, J.; Yaxley, J.; Coomer, J.; Lavin, M. F.; Gardiner, R. A.; Watters, D. Evaluation of the potential of transferrin-adriamycin conjugates in the treatment of bladder cancer. *Br. J. Urol.* **1998**, *82* (2), 284–289.

(41) Kratz, F.; Roth, T.; Fichiner, I.; Schumacher, P.; Fiebig, H. H.; Unger, C. In vitro and in vivo efficacy of acid-sensitive transferrin and albumin doxorubicin conjugates in a human xenograft panel and in the MDA-MB-435 mamma carcinoma model. *J. Drug Targeting* **2000**, *8* (5), 305–318.

## Conclusions

In this work, PAMAM-PEG-T7 was successfully synthesized. The model drug, DOX, could be easily encapsulated in the interior region of PAMAM. This novel nanocarrier showed a promising targeting capability to the transferrin receptor overexpressed tumor in vivo. In addition, the T7-modified drug delivery system could internalize into tumor cells with the help of Tf and accumulate into tumor tissues efficiently after intravenous administration. The antitumor effect of this system was evident even at very low dose. It suggested that T7 can be used as a potent ligand for designing of drug delivery systems targeting transferrin receptor overexpressed tumors.

**Acknowledgment.** This work was supported by grants from the National HighTechnology Research and Development Program ("863"Program) of China (2008AA02Z117), National Basic Research Program of China (973 Program) (2007CB935802), National Natural Science Foundation of China (30901861), and "Key new drug creation program" 2009ZX09310-006.

**Supporting Information Available:** Data of the entrapment efficiency, atom force microscopy, DSC, and dynamic light scattering are tabulated. This material is available free of charge via the Internet at http://pubs.acs.org.

MP100185F